EVALUATION METHOD OF TSUNAMI WAVE PRESSURE ACTING ON LAND STRUCTURE USING 2D DEPTH-INTEGRATED FLOW SIMULATION

Tsuyoshi Arimitsu[1], Kazuya Ooe[2], Koji Kawasaki[3]

Abstract

To design and construct land structures resistive to tsunami wave force, it is most essential to evaluate tsunami pressure quantitatively. The existing hydrostatic formula, in general, tended to underestimate tsunami wave pressure under the condition of inundation flow with large Froude number. Estimation method of tsunami wave pressure acting on a land structure was proposed using inundation depth and horizontal velocity at the front of the structure, which were calculated employing a 2D depth-integrated flow model based on the unstructured grid system. The comparison between the numerical and experimental results revealed that the proposed method could reasonably reproduce the vertical distribution of the maximum tsunami pressure as well as the time variation of the tsunami wave pressure exerting on the structure.

Key words: Tsunami wave pressure, land structure, inundation depth at the front of structure, hydraulic experiment, 2D depth integrated flow simulation

1. Introduction

Previously, the principal approach taken in the design of the power stations has been to prevent any impacts on the plant safety functions by the design-basis tsunami, by ensuring the height of the ground on which the central facilities are located higher than the design-basis tsunami. However, at the time of the 2011 off the Pacific Coast of Tohoku Earthquake, some power stations were challenged by a tsunami that was far beyond the design basis. Even when a design-basis tsunami is derived accordingly with scientific rationality, however, the possibility would remain that an even higher tsunami could come. Therefore, measures against the beyond-design basis tsunami should be based on the consideration of the detailed tsunami behavior. The flooding behavior of tsunami around the facilities within the site should be predicted to support planning for minimizing the damage to structures, systems and components due to the hydrodynamic impacts and forces.

To design and construct structures to stand against the tsunami, evaluation of tsunami wave force acting on the structures is most essential. Asakura et al. (2000) propose the formula (Asakura formula) to evaluate tsunami wave pressure distribution on a land structure and this formula is used for designing a tsunami evacuation building (Japanese Cabinet Office, 2005). The design tsunami wave pressure distribution along the structure's height is assumed a triangular shape with the height reaching three times of inundation depth where no structure exists and the wave pressure at the bottom is assumed to be three times of the hydrostatic pressure. In previous studies, in order to evaluate tsunami wave pressure, tsunami inundation depth has been calculated by using 2-dimensional depth-integrated flow model without land structures and design tsunami wave pressure has been calculated by substituting inundation depth where no structure exists into Asakura Formula. However, if tsunami inundation simulation with consideration of individual land structures is conducted, inundation depth where no structure exists has to be calculated separately.

Therefore, the purpose of this study is to newly propose the estimation method of tsunami wave pressure acting on a land structure making use of 2D depth-integrated flow simulation under the installation of the structure.

[1]The Kansai Electric Power Co., Inc., 3-11-20, Nakoji, Amagasaki, 661-0974, Japan, arimitsu.tsuyoshi@d3.kepco.co.jp
[2]The Kansai Electric Power Co., Inc., 3-11-20, Nakoji, Amagasaki, 661-0974, Japan, ooe.kazuya@d3.kepco.co.jp
[3]Dept. of Civil Engineering, Nagoya Univ., C1-3(651), Furo-cho, Chikusa-ku, Nagoya, 464-8603, Japan, kawasaki@nagoya-u.jp

2. Hydraulic Experiments

2.1. *Experimental setup and conditions*

Hydraulic experiments were conducted to estimate tsunami wave pressure acting on several different types of land structures and examine the influence of a seawall in front of the structure on tsunami wave pressure. The experiments were conducted in a flume which is 18.0m in length, 0.5m in height, and 0.5m in width in the Kansai Electric Power. Figure 1 is a schematic of the experimental set-up. The flume was partitioned to create a testing zone and a reservoir. A gate was installed in order to impound a specified depth of water. The land structure was placed on the flat land section. By a rapid opening of the gate, tsunami propagated through the flume and impacted the land structure. Pressure sensors were placed on the front face of the structure to measure the vertical pressure distribution. Inundation depth and horizontal velocity at the front of the structure were also measured.

The experimental conditions are shown in Table 1. This study used two models of land structures, the width of which are 0.5m and 0.1m, respectively. We varied a distance between a seawall and the structure, seawall height and impoundment depth in the reservoir. The structures were made of acryl plates. Pressure transducers were placed on the front of the model to measure the vertical pressure distribution. Wave gauges measured the wave profile offshore and inundation depth onshore with and without a structure. Propeller current meter determined velocity. The measured data were digitized at the time interval of 0.002s (500 Hz).

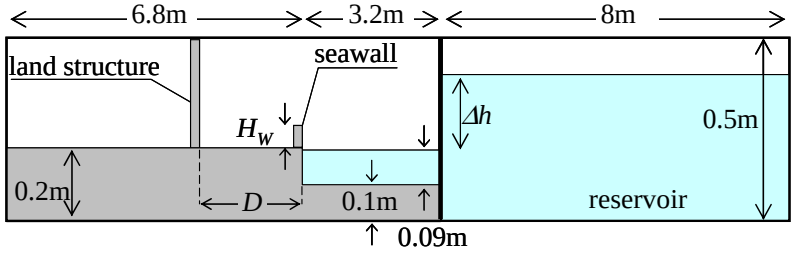

Figure 1. Experimental set-up.

Table 1. Experimental conditions.

Structure	Distance from seawall D(m)	Height of seawall H_W(m)	Impoundment depth Δh(m)
Vertical wall (H=0.30m,W=0.5m - the flume width)	1.0	0	0.18, 0.24, 0.30
		0.02	0.18, 0.24
		0.05	0.24
Rectangular structure (H=0.30m,W=0.1m, L=0.07m)	2.0	0	0.18, 0.24, 0.30
		0.02	0.18, 0.24
		0.05	0.24

2.2. *Experimental results*

2.2.1. *Inundation depth*

Figure 2 provides the time histories of inundation depth h_i, horizontal velocity u_i and Froude number F_r of progressive wave measured at D=1m under the condition of Δh=0.15m. F_r is calculated by the following equation.

$$F_r = u_i \Big/ \sqrt{g h_i} \tag{1}$$

where g is acceleration due to gravity.

The origin of the horizontal axis shows the time when tsunami reached 2 meters off the seawall. In the following, 2 seconds since water level begin to rise and subsequent part with approximately-constant water level were defined here as the leading edge and the main body, respectively. The leading edge of tsunami had small inundation depth and high velocity. On the other hand, at the main body of tsunami, the inundation depth increased and the velocity decreased. Inundation depth and velocity of the leading edge of progressive wave after overtopping of seawall (H_W=0.02cm, 0.05cm) were the same as those without the presence of seawall (H_W=0cm). Seawall could reduce inundation depth at the main body. However, it could not decrease velocity at the main body. As a result, the F_r reached the maximum at the leading edge and decreased in the main body. The main body of tsunami with larger F_r occurred in the case of higher seawall. In particular, in the case of H_W=0.05m, tsunami inundation flow with F_r around 2.0 persisted over a long time. Tsunami inundation flow behind the seawall with insufficient height had the potential of large Froude number.

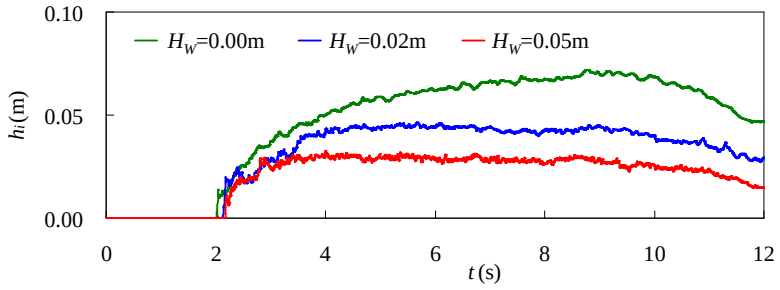

(a) Inundation depth

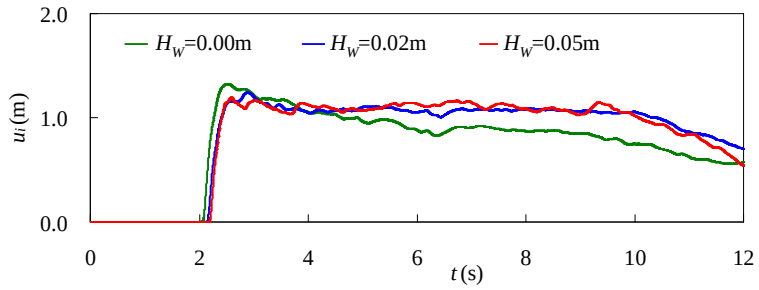

(b) Horizontal velocity

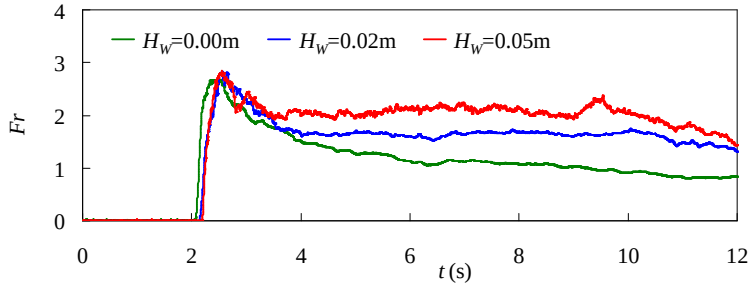

(c) Froude number

Figure 2 Time histories of tsunami inundation flow without the presence of land structure

Figure 3 provides the time series of inundation depth measured at the front of a rectangular structure that is placed at D=1m under the condition of Δh=0.15m. The origin of the horizontal axis shows the time when tsunami reached the structure. The first sudden rise in the inundation depth is due to the initial impact of the leading edge on the structure. While the main body acts on the structure (t >0.2s), tsunami maintains a relatively constant inundation depth. Seawall has no effect on the peak of water level and little effect on the water level of the main body.

As mentioned above, the effect of seawall on the inundation depth varies depending on the presence or absence of the land structure. Therefore, the effect of the land structure should be considered in evaluating tsunami wave pressure acting on the structure.

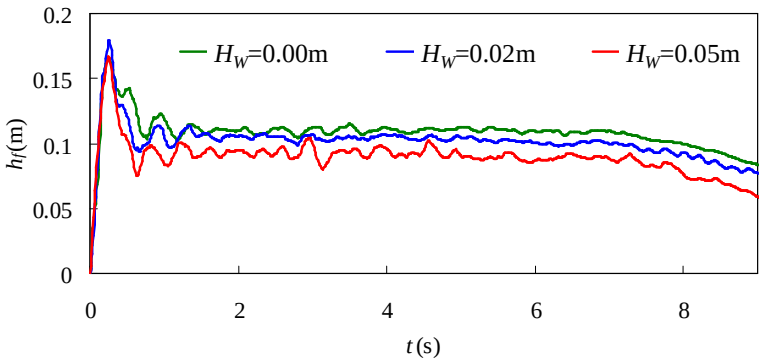

Figure 3 Time histories of inundation depth at the front of structure

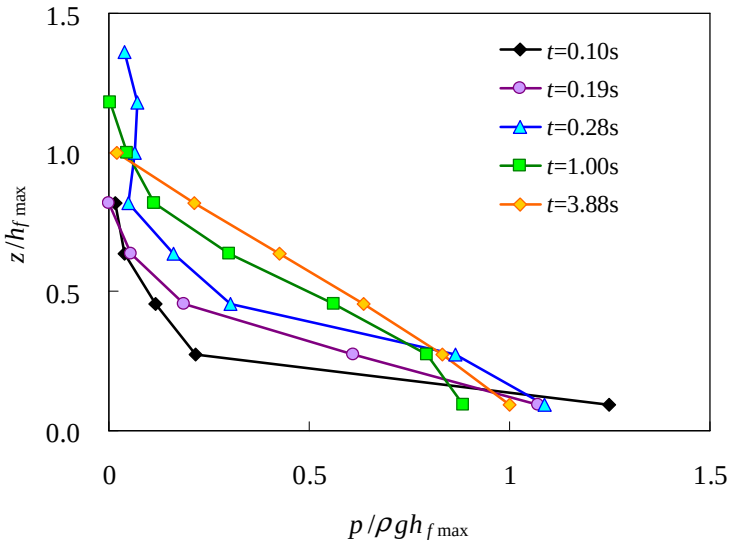

Figure 4 Vertical distribution of tsunami wave pressure for each instant of time

2.2.2. *Tsunami wave pressure*

Figure 4 provides the vertical distributions of dimensionless tsunami wave pressure for each instant of time. Tsunami wave pressure is normalized by the maximum inundation depth $h_{f\max}$ at the front of the structure except the short peak at the leading edge. In this figure, t=0.0s is the time when tsunami reaches the structure. Large pressure occurred near the ground, immediately after tsunami reaching the structure (t=0.1s). The vertical distribution of the pressure was significantly different from the hydrostatic pressure for the equivalent inundation depth. It is due to small inundation depth and high velocity at the leading edge of tsunami. The highest water level due to the initial impact of the leading edge on the structure could

be seen at t=0.28s. At this time, the vertical distribution of the pressure was also different from the hydrostatic pressure for the equivalent inundation depth. When the main body of tsunami acted the structure (t=3.88s), the hydrostatic pressure distribution for the equivalent inundation depth could be seen. Wave pressure at the time of highest water level (t=0.28) was smaller than that of the main body of tsunami (t=3.88s). There is a possibility that tsunami wave with splash may have a less effect on the stability of the structure than that with the main body.

Figure 5 shows the vertical distributions of the maximum tsunami wave pressure. In the case of large impoundment depth, high inundation depth and large pressure occur. Under the conditions in this study, the seawall has little effect of decreasing tsunami wave pressure.

Figure 6 shows the vertical distribution of the maximum dimensionless tsunami wave pressure. Vertical location and the maximum tsunami wave pressure are normalized by the maximum inundation depth h_{imax} without the presence of the structure. A black line connecting 3 times of the inundation depth where no structure exists and 3 times of the hydrostatic pressure shows the result of Asakura formula. The calculation results of Asakura formula can keep on the safe side in the absence of seawall (H_W=0.00m) and are coincident with the experimental data in the case of a low seawall (H_W=0.02m). On the other hand, under the condition of overflow beyond seawall of H_W=0.05m, the calculation results of Asakura formula tends to underestimate tsunami wave pressure. This is because pressure comparable to the case without seawall acts on the structure although inundation depth behind the seawall became smaller than that without seawall.

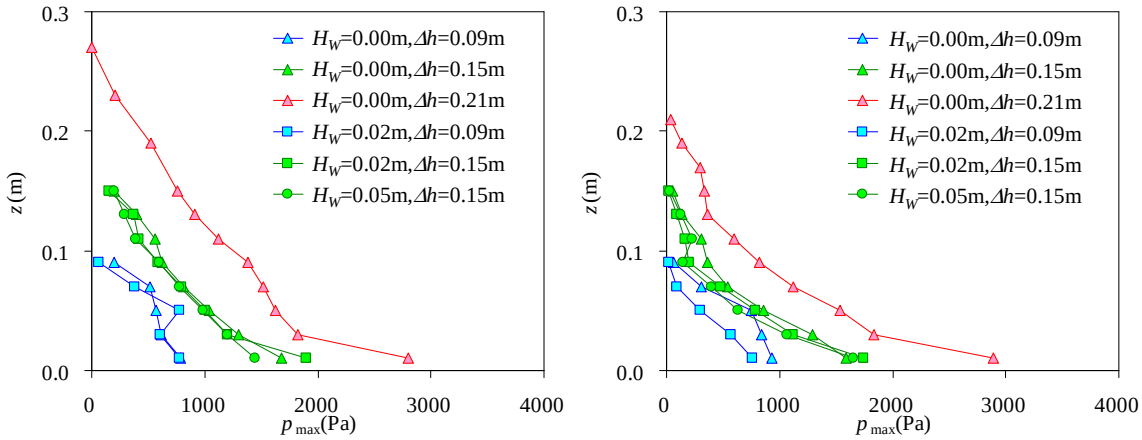

(a) vertical wall (b)rectangular structure

Figure 5 Vertical distribution of the maximum tsunami wave pressure

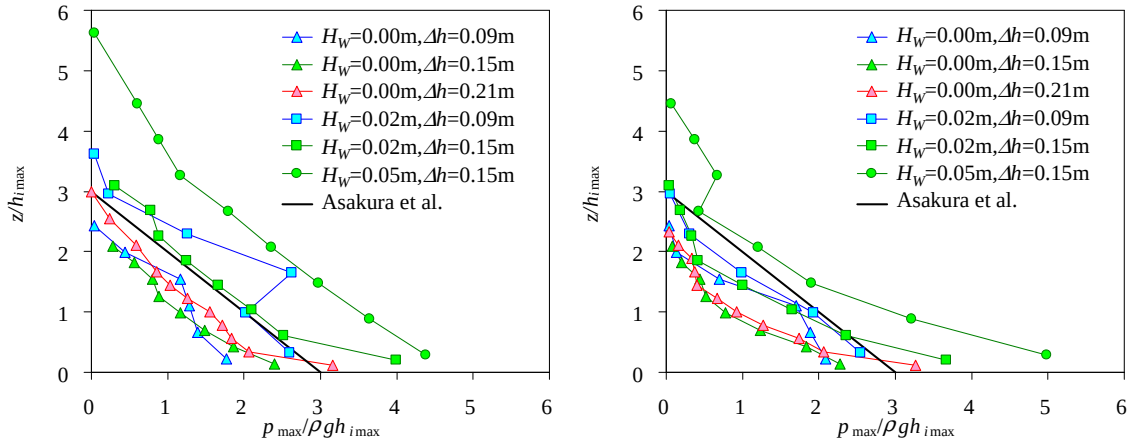

(a) vertical wall (b) rectangular structure

Figure 6 Vertical distribution of the maximum dimensionless tsunami wave pressure

3. Evaluation Method of Tsunami Wave Pressure

3.1. *2D Depth-integrated Flow Simulation*

A 2D model based on the unstructured grid system is used to calculate tsunami inundation. The following 2D shallow water equation is used as the governing equation.

$$\frac{\partial \mathbf{U}}{\partial t}+\frac{\partial \mathbf{E}}{\partial x}+\frac{\partial \mathbf{G}}{\partial y}=\mathbf{S} \tag{2}$$

where **U** is flow vector, **E** and **G** are flux vectors, **S** is vector containing source and sink terms. These vectors are given by

$$\mathbf{U}=\begin{pmatrix} h \\ uh \\ vh \end{pmatrix},\quad \mathbf{E}=\begin{pmatrix} uh \\ u^2h+\dfrac{gh^2}{2} \\ uvh \end{pmatrix},\quad \mathbf{G}=\begin{pmatrix} vh \\ uvh \\ v^2h+\dfrac{gh^2}{2} \end{pmatrix},\quad \mathbf{S}=\begin{pmatrix} 0 \\ gh\left(S_{ox}-S_{fx}\right) \\ gh\left(S_{oy}-S_{fy}\right) \end{pmatrix} \tag{3}$$

where h is water depth, u and v are velocity components along x- and y- direction, respectively, S_{ox} and S_{oy} are bed slopes along x- and y- direction, respectively, S_{fx} and S_{fy} are friction slopes along x- and y= direction, respectively. The bed slopes S_{ox} and S_{oy} are defined as

$$S_{ox}=-\frac{\partial z_b}{\partial x};\quad S_{oy}=-\frac{\partial z_b}{\partial y} \tag{4}$$

where z_b is bed elevation.
The friction slopes S_{fx} and S_{fy} are given by Manning's formula as

$$S_{fx}=\frac{n^2u\sqrt{u^2+v^2}}{h^{4/3}};\quad S_{fy}=\frac{n^2v\sqrt{u^2+v^2}}{h^{4/3}} \tag{5}$$

where n is Manning's roughness coefficient.
The integral form of the governing equations is obtained by integrating Eq. (2) over a control volume Ω using the Gauss divergence theorem as

$$\int_{\Omega}\frac{\partial \mathbf{U}}{\partial t}d\Omega+\int_{\Omega}\nabla\cdot\mathbf{F}d\Omega=\int_{\Omega}\mathbf{S}d\Omega \tag{6}$$

The unstructured finite volume method and a forward Euler method are used to integrate Eq. (6).
The numerical flux is calculated by flux-difference splitting scheme. The bed slope is discretized in the same way as the flux. S_{oi} is written as

$$S_{oi}=\sum_{k=1}^{N_i}\left[\frac{1}{2}L_{i,k}\sum_{m=1}^{3}\left(1-\frac{\left|\tilde{\lambda}_m\right|}{\tilde{\lambda}_m}\right)\tilde{\beta}_m\tilde{\mathbf{e}}_m\right]_i \tag{6}$$

where N_i is total number of cell face (N_i=4 in case of quadrangle cell), $L_{i,k}$ is length of kth cell, λ_m and e_m are the eigenvalues and eigenvectors of the approximate Jacobianis, respectively, and β_m is the coefficients, as follows.

$$\tilde{\mathbf{e}}^1 = \begin{pmatrix} 1 \\ \tilde{u} + \tilde{c} n_x \\ \tilde{v} + \tilde{c} n_y \end{pmatrix}, \quad \tilde{\mathbf{e}}^2 = \begin{pmatrix} 0 \\ -\tilde{c} n_y \\ \tilde{c} n_x \end{pmatrix}, \quad \tilde{\mathbf{e}}^3 = \begin{pmatrix} 1 \\ \tilde{u} - \tilde{c} n_x \\ \tilde{v} - \tilde{c} n_y \end{pmatrix} \tag{7}$$

$$\tilde{\lambda}_1 = \tilde{u} n_x + \tilde{v} n_y + \tilde{c} \ , \quad \tilde{\lambda}_2 = \tilde{u} n_x + \tilde{v} n_y \ , \quad \tilde{\lambda}_3 = \tilde{u} n_x + \tilde{v} n_y - \tilde{c} \tag{8}$$

$$\begin{pmatrix} \tilde{\beta}_1 \\ \tilde{\beta}_2 \\ \tilde{\beta}_3 \end{pmatrix} = \begin{pmatrix} -\frac{\tilde{c}}{2} \Delta z_b \\ 0 \\ \frac{\tilde{c}}{2} \Delta z_b \end{pmatrix} \tag{9}$$

where (n_x, n_y) is the unit outward normal, $(\tilde{u}, \tilde{v}, \tilde{c})$ is the Roe-averaged values. The friction slope is estimated by using **U** defined at the center of each cell.

3.2. *Tsunami Wave Pressure Acting on Land Structure*

Evaluation method is derived based on experimental data. Tsunami wave pressure is obtained as a sum of hydrostatic pressure for the equivalent inundation depth and pressure based on the conservation of momentum (Eq. (10)).

$$p(z,t) = \rho g \{ h_f(t) - z \} + \rho u_f(t)^2 \tag{10}$$

where z is vertical distance, t is time, p is tsunami wave pressure, ρ is density of water, h_f is inundation depth at the front of structure, u_f is horizontal velocity at the front of structure.

Figure 7 illustrates the concept employed in Eq. (10). When the leading edge acts on the structure, small hydrostatic pressure and large pressure based on the conservation of momentum occur. On the other hand, large hydrostatic pressure and small pressure based on the conservation of momentum occur when the main body of tsunami acts on the structure.

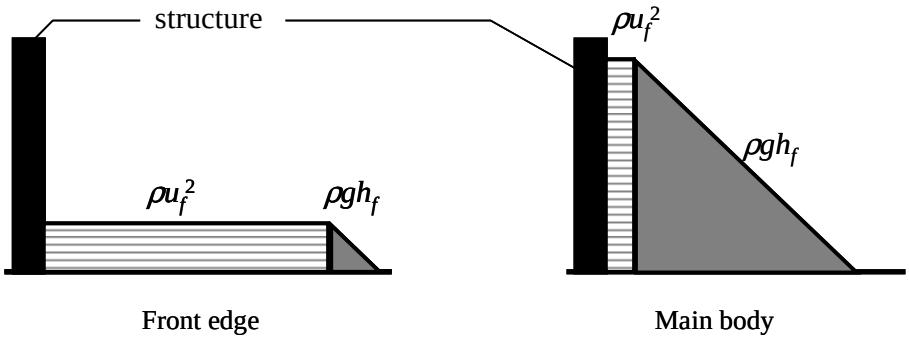

Figure 7 Concept employed in the proposed method

4. 2D Depth-Integrated Flow Simulation

4.1. *Tsunami Inundation Flow*

To perform the comparison of the experimental and numerical results, the experimental geometry was represented in the numerical model. The initial water depth was set as same as the hydraulic experiments.

Variable grid size was applied to the computation domain with the cross-shore grid size (*dx*) of 0.03~0.01m and alongshore grid size (*dy*) of 0.01m.

Figure 8 (a) and (b) show the comparison between calculation and experimental results on time series of inundation depth where no structure exist and at the front of a rectangular structure, respectively. The numerical model gives satisfactory accurate prediction of inundation depth of progressive tsunami wave. Because of 2D model, splash due to the initial impact of the leading edge on the structure cannot be reproduced by the simulation. However, the calculation results are in good agreement with the experimental ones except the highest water level.

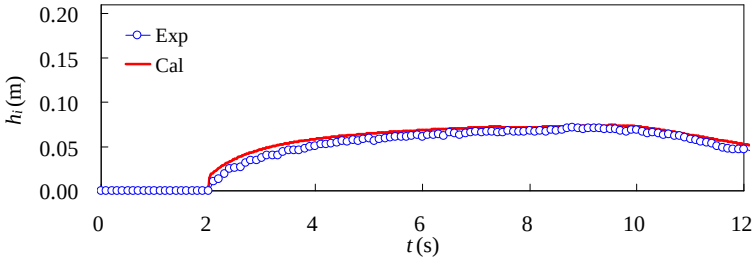

(a) Inundation depth where no structure exist

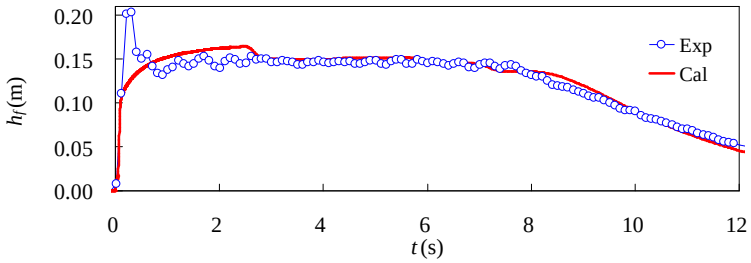

(b) Inundation depth at the front of structure

Figure 8 Comparison between numerical and experimental results in terms of time history on inundation depth

4.2. *Tsunami Wave Pressure Acting on the Structure*

Comparison between the proposed method and the experimental result on the vertical distributions of the maximum dimensionless tsunami wave pressure acting on the vertical wall is shown in Figure 9. The maximum inundation depth h_{imax} where no structure exists is used for normalization. Calculated result was different from the hydrostatic pressure distribution because pressure near the bottom is large. The proposed method can reproduce the experimental result by considering peak pressure due to leading edge of tsunami in second term on the right hand side in Eq. (10). In consequence, the proposed equation can make a rational evaluation of tsunami wave pressure.

Figure 10 shows comparison between the proposed method and the experimental result on the vertical distributions of the maximum dimensionless tsunami wave pressure acting on the rectangular structure. Because water level dammed by the rectangular structure was lower than that by vertical wall, a part of tsunami wave pressure that shows hydrostatic pressure distribution acting on the rectangular structure is smaller than that on the vertical wall. On the other hand, there is not much difference in terms of the maximum wave pressure near the ground between the two structures because impulsive pressure caused by leading edge does not depend on the width of structure.

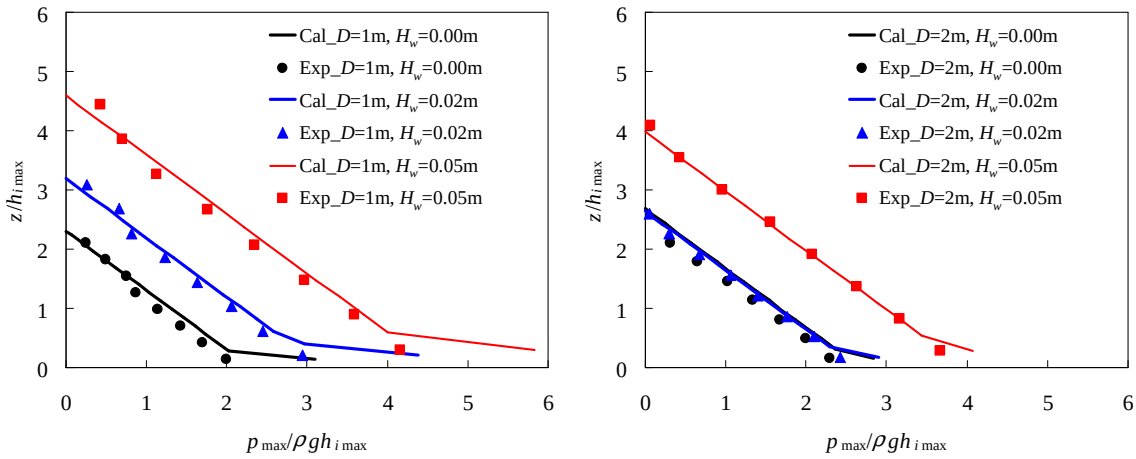

(a) D=1m (b) D=2m

Figure 9 The maximum tsunami wave pressure distribution acting on vertical wall

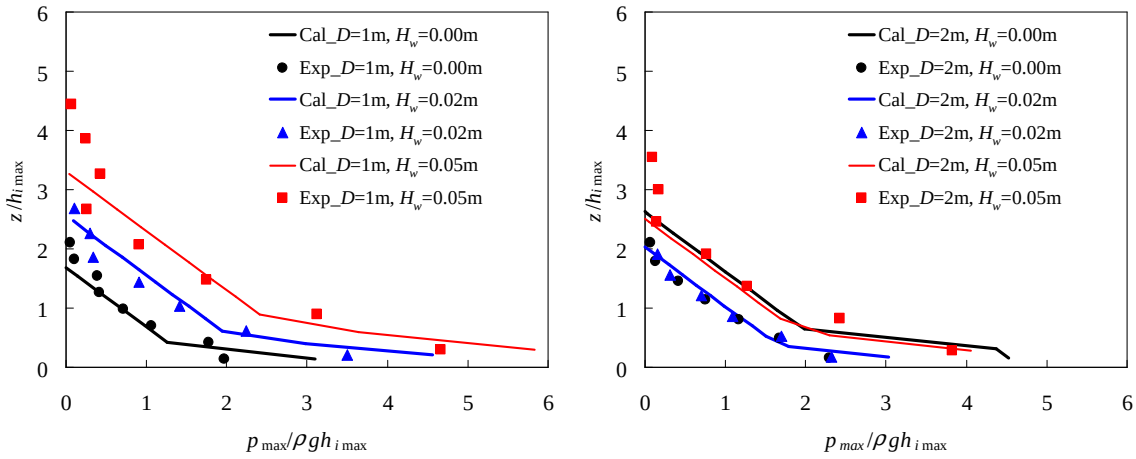

(a) D=1m (b) D=2m

Figure 10 The maximum tsunami wave pressure distribution acting on rectangular structure

5. Conclusion

This study proposed the evaluation method of tsunami wave pressure acting on a land structure by using inundation depth and horizontal velocity at the front of the structure. The wave pressures estimated by Eq. (10) were compared with the measured wave pressures.

The obtained results are summarized as follows:

(1) The comparison between the numerical and experimental results revealed that the proposed method could reasonably reproduce the maximum tsunami pressure, as compared with the proposed formula by Asakura et al. (2000).

(2) Tsunami wave pressure after overtopping on the seawall was rarely different from that without seawall. On the other hand, inundation depth behind the seawall became smaller than that without seawall. In consequence, Asakura formula tended to underestimate tsunami wave pressure under the condition of overtopping on seawall.

Acknowledgements

The authors gratefully acknowledge Mr. Hiroshi Uchinishi and Mr. Hirokazu Ikeda, Japan Industrial Testing Corporation, for their important contributions to the experiments.

References

Asakura, R., Iwase, K., Ikeya, T., Takao, M., Kaneto, T., Fujii, N., and Ohmori, M., 2000. Experimental Study on Wave Force Acting on On-shore Structures due to Overflowing Tsunamis, *Proceedings of Coastal Engineering, Japan Society of Civil Engineers*, 47, 911-915 (in Japanese).

Japanese Cabinet Office, 2005. *Guideline for Tsunami Evacuation Building*, http://www.bousai.go.jp/oshirase/h17/050610/guideline.pdf (in Japanese).